PROTEINS: Structure, Function, and Genetics 16:226–245 (1993)

Absolute and Relative Binding Free Energy Calculations of the Interaction of Biotin and Its Analogs With Streptavidin Using Molecular Dynamics/Free Energy Perturbation Approaches

Shuichi Miyamoto and Peter A. Kollman
Department of Pharmaceutical Chemistry, University of California, San Francisco, California 94143

ABSTRACT **We present calculations of the absolute and relative binding free energies of complexation of streptavidin with biotin and its analogs by means of a thermodynamic free energy perturbation method implemented with molecular dynamics. Using the recently solved crystal structure of the streptavidin–biotin complex, biotin was mutated into a dummy molecule as well as thiobiotin and iminobiotin both in the protein and in solution. The calculated absolute binding free energy was dependent on the simulation model used. Encouragingly, the "best models" provided a reasonable semiquantitative reproduction (−20 to −22 kcal/mol) of the experimental free energy (−18.3 kcal/mol). Furthermore, the calculated results give clear insights into the binding nature of the protein–ligand complex, showing that the van der Waals energy dominates the electrostatic and hydrogen bonding energies in the binding of biotin by streptavidin. Specifically, the mutation of biotin into a dummy molecule in solution has a ΔG (van der Waals) ~ −4 kcal/mol, due to the cancellation of dispersion and repulsion "cavity" effects. On the other hand, in the protein, a very small free energy price must be paid to create a cavity since one already exists and the mutation of biotin into a dummy molecule has a ΔG (van der Waals) ~ 15 kcal/mol. These results are also consistent with the interpretation that the entropy increase to be expected from hydrophobic interactions from desolvation of biotin is counterbalanced by a decrease in entropy accompanying the formation of buried hydrogen bonds, which have been derived from the apparently conflicting experimental data. They provide an alternative interpretation of the reason for the extremely high affinity of the biotin–streptavidin interaction than that recently proposed by Weber et al. (J. Am. Chem. Soc. 114:3197, 1992). In the case of the relative binding free energies, the calculated values of 3.8±0.6 and 7.2±0.6 kcal/mol compare well with the experimental values of 3.6 and 6.2 kcal/mol for the perturbation of biotin to thiobiotin and iminobiotin, respectively in the related protein avidin. The calculations indicate that desolvation of the ligand is important in understanding the relative affinity of the ligands with the protein. The above successful simulations suggest that the molecular dynamics/free energy perturbation method is useful for understanding the energetic features affecting the binding between proteins and ligands, since it is generally difficult to determine these factors unambiguously by experiment. This set of studies provide a textbook example of the key elements of protein–ligand recognition: the electrostatic free energy dominates the relative affinities, the van der Waals free energy dominates the absolute free energy; the free energy of desolvation is a key to why iminobiotin is so much more weakly bound than biotin and the free energy of binding explains why thiobiotin is so weakly bound relative to biotin.**

Key words: molecular dynamics, biotin, avidin, free energy calculations

INTRODUCTION

The binding of biotin by avidin is accompanied by one of the largest decreases in free energy yet observed for a noncovalent interaction between a protein and a small ligand in aqueous solution. Avidin and the homologous protein streptavidin are tetrameric proteins (MW = 4 × 15,000) and bind up to four molecules of biotin. The dissociation constants for the protein–ligand complexes are on the order of 10^{-15} M and the complexes are extremely stable over a wide range of temperature and pH.[1] Although the biological functions of avidin and streptavidin are poorly understood, these proteins may function as antibiotics that deplete the environment of the essential vitamin biotin. Interest in the avidin family, however, transcends their natural biology. They have been studied primarily to understand the

Received January 7, 1993; accepted January 27, 1993.
Address reprint requests to Dr. Peter A. Kollman, Department of Pharmaceutical Chemistry, University of California, 513 Parnassus Ave., San Francisco, CA 94143.

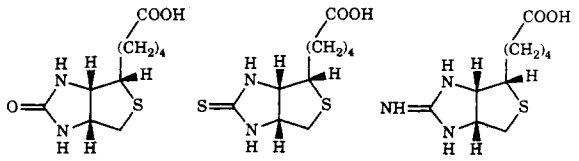

Fig. 1. Chemical structures of biotin and its analogs.

chemical and structural basis for the high affinity. At the same time, their remarkable binding ability for biotin has led the attempts to optimize biotechnology applications that exploit this activity.[2]

Very recently the three-dimensional structures of streptavidin, with and without biotin, have been determined by X-ray crystallography.[3] Streptavidin is isolated from the actinobacterium *Streptomyces avidinii*.[4] The crystal structure has been solved for the core streptavidin, which consists of residues 15 through 133 of native 159-residue streptavidin chain in the case of the protein–ligand complex. This core streptavidin shares 38% sequence identity[5] with avian egg white avidin and retains full biotin-binding activity. The streptavidin protomer is organized as an 8-stranded β-barrel. Pairs of the barrels hydrogen bond together to form symmetric dimers. The naturally occurring streptavidin tetramer is formed by interdigitating a pair of dimers with their dyad axes coincident. Biotin binds in a pocket at one end of each barrel.

Numerous hydrogen-bonding (H-bonding) and van der Waals (VDW) interactions are involved in the biotin binding. These include five hydrogen bonds to the biotin ureido group. Three side chain atoms, Asn-23HN$^{\delta 2}$, Ser-27HO$^{\gamma}$, and Tyr-43HO$^{\eta}$, are situated in a position to hydrogen bond with the ureido oxygen. Ser-45O$^{\gamma}$ and Asp-128O$^{\delta 2}$ interact with each of ureido HM, respectively. Two additional hydrogen bonds are formed with the valeryl carboxyl group of biotin. Four tryptophans are in contact with each biotin molecule Nearly all of the interactions are from the residues of a given subunit, and residues from seven β-strands and two loops contribute directly to the binding. However, one of the tryptophans (Trp-120) is supplied by the dyad-related subunit. As a consequence of this extensive pattern of interactions, resulting in part from the ordering of loop Ser-45 to Ala-50, bound biotin is essentially buried in the pocket with only the valeryl carboxyl oxygens and one NH group partially accessible to solvent. Comparison of streptavidin and avidin shows that all of the groups that directly bind biotin are conserved, with the exception of Ser-45 and Asp-128, which are replaced by the residues with similar functionality.

It appeared to us that the streptavidin–biotin complex was a good model with which to begin examining the basis for the extremely high affinity between protein and ligands using a computational method. The binding free energies of biotin and a couple of congeners by avidin were experimentally determined from the dissociation constants at 25°C and are −20.5 (biotin), −16.9 (thiobiotin), and −14.3 (iminobiotin) kcal/mol while that of biotin by streptavidin is −18.3 kcal/mol.[3b] The structures of these ligand molecules are shown in Figure 1. It was challenging to calculate a large free energy change of a complex ligand binding to a complex protein with a computational approach. Moreover, there were conflicting interpretations of the nature of the strong association, although the relation of affinity to ligand structure had been well studied by the binding experiments with biotin and more than two dozen analogs. Spectroscopic studies of the complexation led to the conclusion that hydrophobic interactions made a large contribution to the free energy of binding,[7,8] although calorimetric studies suggested that the combination of avodin with biotin is accompanied by no net change of entropy and a large decrease in enthalpy.[6] The goal of this study is to see whether the free energy perturbation (FEP) method can yield qualitative insight into the ligand binding and to see how well this method can reproduce the quantitative data from the experimental studies.

The FEP method had its roots many years ago, but the generalization of the method and its incorporation into a molecular simulation program were stimulated by the implementation by Postma et al.[9] and others.[10] A description of this implementation was given by Singh et al.[11] and earlier applications to molecular solvation, protein–ligand binding and enzyme catalysis were presented by Bash et al.[12] and Rao et al.[13] More recently the approach has been applied to investigate many processes involving complex macromolecular systems and, so far, the results are encouraging.[14]

In this study, we apply the FEP theory in an attempt to calculate the absolute and relative binding free energies of complexation of streptavidin with biotin and its analogs, thiobiotin and iminobiotin. The calculated results are in generally reasonable semiquantative agreement with experiment. To our knowledge this is one of the first successful computational studies on the absolute binding free energy of complexation of a protein and a very complex organic molecule as a ligand although Hermans and Shankar studied Xe binding to myoglobin,[15] Merz has studied CO_2 binding to carbonic anhydrase,[16] and Lee et al. phosphoryl choline analogs to McPC603.[17] Specifically, it has become clear that van der Waals (hydrophobic) interactions play an important role in binding of biotin by streptavidin. In the case of the relative binding free energy calculations, an almost quantitative level of agreement with related experiments is obtained and the results

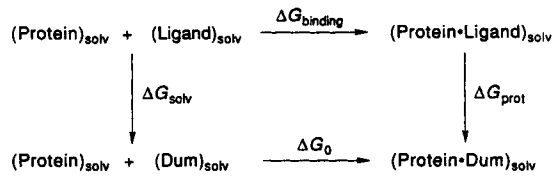

$$\Delta\Delta G_{bind} = \Delta G_{binding} - \Delta G_0 = \Delta G_{solv} - \Delta G_{prot}$$

Scheme 1.

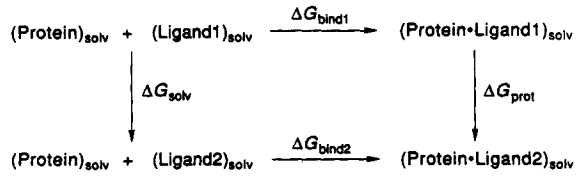

$$\Delta\Delta G_{bind} = \Delta G_{bind2} - \Delta G_{bind1} = \Delta G_{prot} - \Delta G_{solv}$$

Scheme 2.

show a critical role of desolvation in understanding molecular association.

METHODS

We used the FEP method to calculate the binding free energy of complexation. This method uses an easily derived equation from classical statistical mechanics to relate the free energy difference between two states to the ensemble average of the potential energy difference between the states. The details have already been presented in the literature.[14] As shown by previous studies,[15–19] this approach can be related to the thermodynamic cycle in Scheme 1, in the case of the absolute binding free energy calculation of the protein–ligand complex. The experimental binding free energy of complexation of streptavidin with biotin, $\Delta G_{binding}$ has been determined to be −18.3 kcal/mol.[3b] ΔG_{solv} is the free energy for mutating the ligand, biotin to a dummy molecule, Dum in solution, which is an estimate for the solvation free energy of biotin. This dummy molecule has all the masses, bond length, angle, and torsional parameters as biotin, but no van der Waals or electrostatic interaction parameters on its atoms. ΔG_{prot} is the change in free energy for the same mutation when the ligand is bound to the protein. The ΔG_{solv} and ΔG_{prot} are calculated by the FEP method.

The entire ligand was treated as the perturbation group and no intraligand free energy changes were considered in the calculation, although the capability to do so is contained in AMBER4.[20] The excellent agreement with experiment found in a wide variety of solvation free energy calculations which assume that the intraligand free energies are the same in the gas phase and solution supports this assumption.[11–13,16–18,21] If the dummy molecule consists of the dummy atoms which have no nonbonded interactions with other atoms (no electrostatic, H-bonding nor VDW energies), ΔG_0 becomes zero. Since the free energy is a state function, the calculated free energy difference $\Delta\Delta G_{bind}$, defined as $\Delta G_{solv} - \Delta G_{prot}$, can be related to the experimentally determined free energy $\Delta G_{binding}$ by the relationship $\Delta\Delta G_{bind} = \Delta G_{solv} - \Delta G_{prot} = \Delta G_{binding} - \Delta G_0 = \Delta G_{binding}$.

Because of the negatively charged carboxyl terminal of biotin, the net molecular charge changes if all atoms of biotin are mutated to dummy atoms. When calculating relative free energy of two species of different charges with a finite Coulombic interaction cutoff such as 8 Å, it is essential to include a correction due to the finite cutoff. Although this correction can be calculated from the Born formula,[22] the Born radius is not well defined in the case of the periodic boundary condition simulations.[23,24] We therefore decided to employ two kinds of dummy molecules. One is a complete dummy molecule composed of all dummy atoms, i.e., complete disappearance of the ligand. The other is a partial dummy molecule in which the negatively charged terminal is left unchanged (Fig. 2). As a consequence, ΔG_0 is no longer equal to zero in the latter case, but the Born correction should not be essential.

In the case of the relative binding free energy calculation of complexation, the thermodynamic cycle in Scheme 2 is employed. The perturbation simulations are carried out by mutating biotin (ligand1) to thiobiotin and iminobiotin (ligand2) both in water and in the protein. There is no need to include the Born correction for those calculations because the total charge of the ligand is conserved during the perturbation. The calculated free energy difference $\Delta\Delta G_{bind}$, defined as $\Delta G_{prot} - \Delta G_{solv}$ should be equal to the relative binding free energy $\Delta G_{bind2} - \Delta G_{bind1}$ derived by experiment.

Before every perturbation calculation the system was energy minimized through molecular mechanical calculations followed by the equilibration at the proper temperature using molecular dynamics. The molecular mechanics, dynamics and FEP calculations were performed with the AMBER package,[20,25] using an all-atom force field. Additional force field parameters used in the present study are given in Table I. Most of them came from analogous parameters provided in the AMBER standard database. Some parameters were based on the X-ray and spectroscopic studies.[26] With respect to the nonbonded parameters (H-bonding and VDW parameters) of an sp2 type sulfur atom, we simply used those of an sp3 type sulfur. In contrast to the sulfurs in cysteine and methionine, no lone pairs were employed on the sulfurs in biotin and its analogs. This is because Jorgensen and Tirado Rives[27] showed

these were not essential in representing solvation properties of sulfur compounds.

The atomic partial charges of the ligand molecules were determined to reproduce the electrostatic potential (surface)[28] obtained from 6-31G* ab initio calculations on the two halves of the molecules, i.e., a bicyclic ring and a side chain using GAUSSIAN 80 UCSF.[29] In both structures the methylene group of the junction (C5) was included as a methyl group and partial charges were adjusted at that part to ensure that the net charge of the biotin molecule becomes −1. These charges and atom types of the ligands are illustrated in Figure 2. The partial charges of the unperturbed atoms of the partial dummy molecule were obtained by slightly modifying those of biotin in order to ensure a net −1 charge for the fragment.

The crystal structure of the streptavidin-biotin complex has been solved to an r factor of 0.172 at 1.55 Å resolution.[3b] The starting structure of the tetrameric complex was built by rotating the X-ray structure of a dimer around the two-fold axis. Histidines 87 and 114 were treated as unprotonated (HID) since the pK_a of the histidine is smaller than the pH at which binding studies were typically done. All Lys and Arg residues were positively charged and Glu and Asp residues were negatively charged. The pH of the crystal structure of the complex was 7.8 and the experimental binding free energies were determined in the range of 5–9 (the complex was extremely stable over a wide pH range). No crystallographic waters were used in the calculations. A spherical cap of 205 TIP3P[30] water molecules within 18 Å of the center of mass of the ligand was added and harmonic radial forces (1.5 kcal/mol·Å^2) were applied to any water leaving this 18 Å boundary.[12a]

One ligand, the protein residues that contain atoms within 12 Å of any atom in the ligand and water molecules were allowed to move with the remainder of the tetramer frozen although still interacting in its nonbonded interactions with the binding site. Any protein residue with all its atoms farther than 15 Å from any atom of a mobile residue were removed from the system to reduce the amount of memory needed for the calculations, with exceptions in order not to break any contiguous protein chain. The binding mode of biotin is illustrated schematically in Figure 3. The initial structure for the determination of ΔG_{solv} was a periodic box containing biotin in the conformation taken from the crystal coordinates and 502 TIP3P water molecules. The initial box dimensions were 18.4 × 25.1 × 25.3 Å.

A constant dielectric of 1.0 was used in all calculations. In the molecular dynamics calculations the SHAKE algorithm[31] was applied to constrain all bonds at their equilibrium lengths and an integration time step of 2 fsec was used unless otherwise specified. The pairlist update was performed every 10 time steps. The free energy perturbations were run with the GIBBS module in the AMBER package.[20]

All perturbation simulations were preceeded by molecular dynamics equilibration, during which the structure, temperature, and total energy were monitored for stability. The backward simulations were also proceeded by a 6 psec equilibration at $\lambda = 0$.

RESULTS

Absolute Binding Free Energy Calculations

Perturbation to the partial dummy molecule

The perturbation of biotin to the partial dummy molecule was carried out using a residue-based nonbonded cutoff of 8 Å. The first simulation was to determine the solvation free energy, ΔG_{solv}. The solvated box system was optimized using energy minimization followed by the equilibration with molecular dynamics for 8 psec at 298 K under periodic boundary conditions at constant pressure (1.0 bar).[23] The resultant equilibrated structure is given in Figure 4. Several test runs of 16 psec in length in the forward direction were initially performed with and without the electrostatic decoupling option using both "windows"[32] and "slow growth"[33] methods to examine the dependence of the free energy on these parameters. Our results indicated that electrostatic decoupling (i.e., the perturbation of electrostatic and H-bonding parameters followed by that of VDW parameters) and the "slow growth" approach gave a more smooth change of free energies. The separate perturbation of the two components of the nonbonded interaction allowed the role of the different contributions to the protein–ligand interactions to be identified as well.

In the above test calculations, we used the GIBBS module of AMBER3A,[20b] in which there is no provision to handle 10–12 interactions between atoms included in the perturbed group and any other atoms. In our case the perturbed group, biotin contains H-bonding donors and acceptors. On the other hand, the newly developed GIBBS module of AMBER4[20c] allows the perturbation of hydrogen bond 10–12 potentials. Therefore, using both of AMBER3A and AMBER4, 60 psec simulations were carried out with the electrostatic decoupling option and the "slow growth" method. In addition, new mixing rules of nonbonded parameters available only in AMBER4, were employed. The new mixing rules are described by[32,34]

$$q_a q_b(\lambda) = \lambda \times q_a(\lambda = 1) q_b(\lambda = 1) + (1 - \lambda) \times q_a(\lambda = 0) q_b(\lambda = 0)$$

$$\varepsilon_{ab}(\lambda) = \lambda \times \sqrt{\varepsilon_a(\lambda = 1)\varepsilon_b(\lambda = 1)} + (1 - \lambda) \times \sqrt{\varepsilon_a(\lambda = 0)\varepsilon_b(\lambda = 0)}$$

$$r^*_{ab}(\lambda) = \lambda \times 1/2 \times [r^*_a(\lambda = 1) + r^*_b(\lambda = 1)]$$

TABLE I. Additional Force Field Parameters Used in This Study*

Bond	K_r (kcal mol^{-1} Å^{-2})	r_{eq} (Å)		
SD–C	395.0	1.69		
Angle	K_θ (kcal mol^{-1} rad^{-2})	θ_{eq} (deg)		
N–C–N	70.0	115.4		
SD–C–N	80.0	122.9		
Dihedral angle	idivf†	$V_n/2$ (kcal mol^{-1})	γ (deg)	n
SD–C–N–X	4	11.2	180.0	2
Improper dihedral angle		$V_n/2$ (kcal mol^{-1})	γ (deg)	n
SD–C–N–N		10.5	180.0	2

*Nonbonded parameters of an sp2 sulfur atom (SD) are not included since those of an sp3 sulfur atom were used for them.
†The factor by which the torsional barrier is divided. It corresponds to the number of torsions associated with the central bond, which is the product of the number of explicit substituents on the two central atoms.

$$+ (1 - \lambda) \times 1/2 \times [r_a^*(\lambda = 0) + r_b^*(\lambda = 0)]$$

$$r_{ab}^*(\text{state where one atom vanishes}) = 0.0$$

while those implemented in AMBER3A are shown by

$$q_a q_b(\lambda) = q_a(\lambda) q_b(\lambda)$$

$$\varepsilon_{ab}(\lambda) = \sqrt{\varepsilon_a(\lambda)\varepsilon_b(\lambda)}$$

$$r_{ab}^*(\lambda) = 1/2 \times [r_a^*(\lambda) + r_b^*(\lambda)]$$

$$r_{ab}^* \text{ (state where one atom vanishes)} = r_a^* \text{ (non-vanishing atom)}$$

where q_a and q_b are partial charges of the interacting atoms a and b, ϵ_a and ϵ_b are the VDW well-depths, and r_a^* and r_b^* are the VDW radii for those atoms.

The new mixing rules available in AMBER4 improved the calculated hysteresis of the total energy. However, individual hystereses of the electrostatic and H-bonding energies and the VDW energy were larger than that of the older mixing rules. It was also found that the free energy did not change monotonically as λ changed. The changes in free energy with λ were greatest near $\lambda = 1$, i.e., where the ligand was most polarized or most massive as shown in Figure 5a. This trend was also observed by Jorgensen et al.[21] and Wade et al.[35] when computing the free energies on mutating methanol into ethane and water into nothing, respectively, in water.

An additional simulation was, therefore, carried out in order to determine a more accurate free energy. This was done similarly to the approach of Eerden et al.[36] or Wade et al.[35] by changing λ slowly with time where the free energy showed greater variation with λ. For example, the simulation time of 15 psec was used in two regions of $\lambda = 1.0–0.75$ and $\lambda = 0.75–0.0$ for the electrostatic and H-bonding perturbation and those of 16 and 32 psec were employed in two parts of $\lambda = 1.0–0.8$ and $\lambda = 0.8–0.0$, respectively, for the VDW perturbation in the case of the forward direction. As a result reasonably small hystereses were obtained (Fig. 5b), giving ΔG_{solv} of 14.5±1.1 kcal/mol. Table II lists the calculated free energies change for biotin → partial dummy molecule in aqueous solution. The solvation free energy of biotin is almost entirely attributable to the electrostatic and H-bonding interactions and the VDW contribution to this free energy is nearly negligible.

The second simulation was to determine the difference in the free energies between the ligand and the dummy molecule bound to the protein (ΔG_{prot}). All protein calculations were carried out using AMBER4.[20c] Following minimization, the solvated protein–ligand system was warmed up and equilibrated using molecular dynamics for 8 psec at 298K. In order to keep the dummy molecule in the binding site, carbon atoms of C2 and C3 (Fig. 3) were constrained by harmonic forces of 10.0 kcal/mol·Å^2 to the locations of the minimized structure during the molecular dynamics simulations. An examination of the structure after equilibration revealed that one of the five hydrogen bonds between the ureido group of the ligand and the protein had been broken. Since those hydrogen bonds were assumed to be important for binding,[1,37] we reran the equilibration in two steps as used in the simulation of subtilisin.[38]

The minimized system was equilibrated for 4 psec with the internal distance restraints on these five hydrogen bonds (2.8 Å, 25 kcal/mol·Å^2) and then equilibrated for an additional 3 psec without restraints. In the resulting structure, all of the five hydrogen bonds were conserved as expected. Thus, we decided to carry out restrained free energy simulations. Another 3 psec equilibration with the weak restraints of 5 kcal/mol·Å^2 was performed starting from the preequilibrated structure for 4 psec with the 25 kcal/mol·Å^2 restraint. The free energy calculations were carried out on these two systems using the "slow growth" method, and the free energies for the forward ($\lambda = 1 \rightarrow 0$) direction were obtained. The electrostatic decoupling option and the new mixing rules of nonbonded parameters were

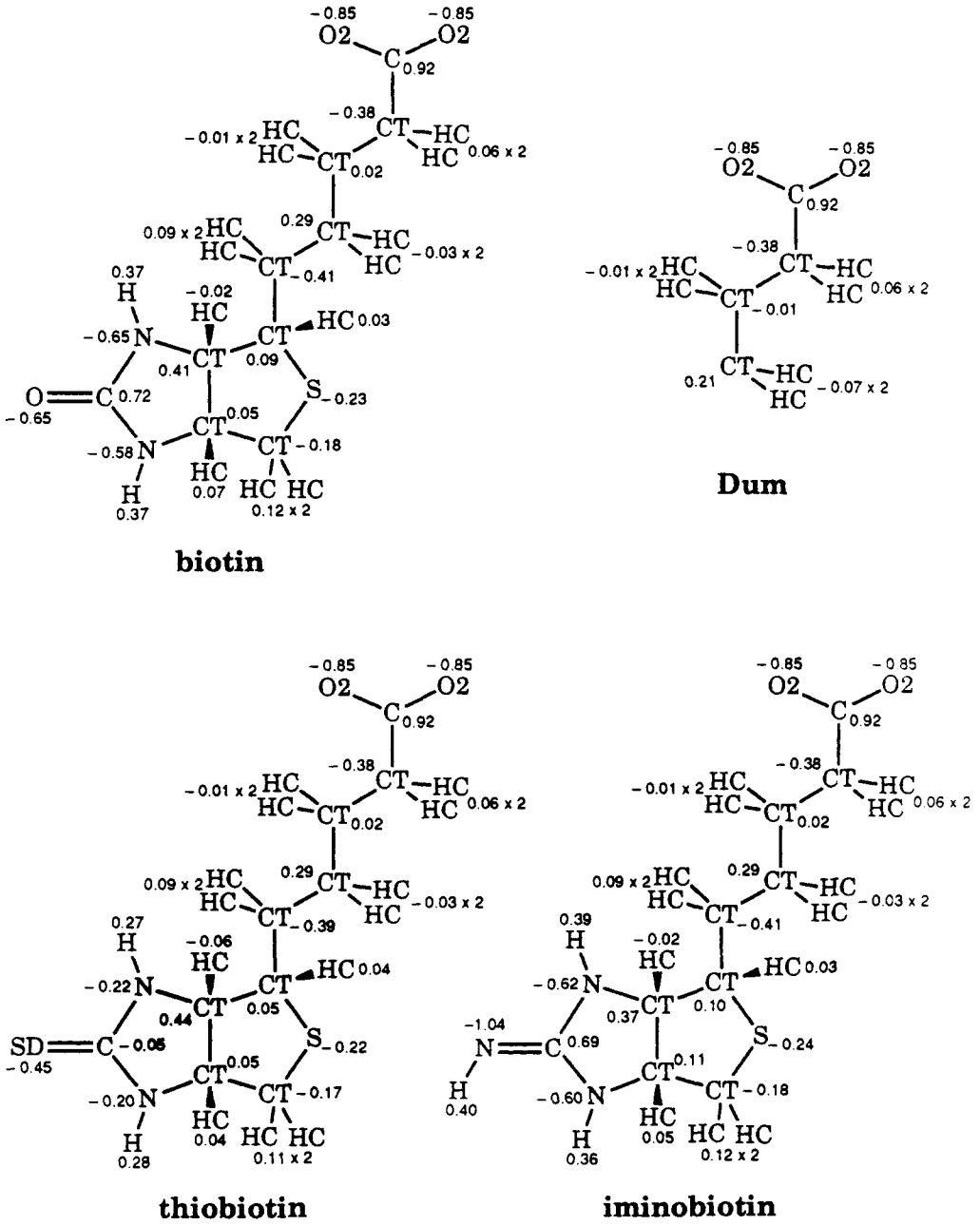

Fig. 2. Partial atomic charges and atom types of the ligands. Dum represents the partial dummy molecule. The complete dummy molecule is not shown since it has no atomic charges.

employed. A pair of the equilibrated and perturbed structures is given in Figure 6.

The calculated free energies for these simulations are presented in Table III. When restraints were applied for the perturbation in the forward direction larger free energy changes were obtained. Whatever the restraint model, the free energy change due to the electrostatic and H-bonding interactions was found to be greater than that of the VDW interactions by about 5 kcal/mol. Although it is difficult how to evaluate or interpret the effect of the restraints on the free energy, we suggest they mainly serve to minimize the drift of the system from the correct experimental structure. The simulated structures were therefore examined to see the conformational effect of the restraints.

In Table IV, we present the root-mean-square (rms) differences between the calculated and the crystal, minimized and equilibrated structures. The deviations were calculated using the nonhydrogen atoms

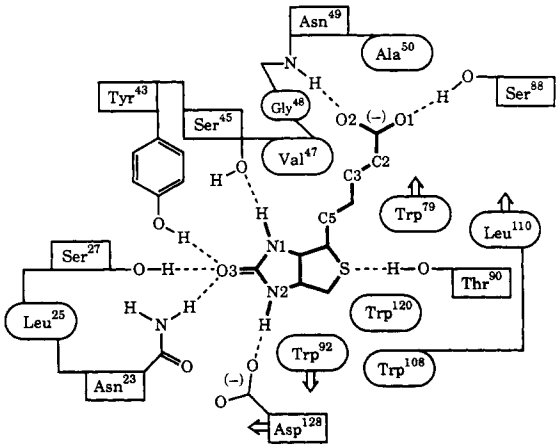

Fig. 3. Schematic representation of the binding mode of streptavidin–biotin. Residues consisting of the hydrogen bonding interactions are indicated by squares. Residues enclosed by ellipsoids represent those involved in van der Waals interactions. Trp-120 is supplied by the dyad-related subunit.

of the protein residues which were allowed to move during the simulations. The comparison to the crystal structure showed that more than half of the movement from the X-ray model occurred upon minimization, although some displacement continued both in equilibration, and during the forward perturbation simulation in both cases (with and without restraints), as were observed in other studies on proteins.[39,40a]

It was also found that the deviation of the perturbed structure (1.49 Å for all non-hydrogen atoms in the case of unrestrained model) from the X-ray structure was much smaller than the sum of the deviation (0.81 Å) of the minimized structure from the X-ray structure and that (1.33 Å) of the perturbed from the minimized. In other words, a certain amount of the movement occurred during the MD simulations without deviating further from the X-ray conformation. The side-chain atoms of Arg-53, Tyr-83, Lys-121, and Glu-116 had large deviations from the X-ray structure after minimization. These atoms moved to form hydrogen bonds to water molecules and had different geometries from that found in the crystal structure.

As one can see in Table IV, the rms deviations of the restrained structures are smaller than those of the corresponding ones without constraints. This feature is clearly observed if the deviations of the perturbed structures ($\lambda = 0$) were compared. For example, the deviations of 1.15 and 1.05 Å (all non-hydrogen atoms) from the X-ray structure and the minimized structure, respectively, for the restraint model are about 0.3 Å smaller than those (1.49 and 1.33 Å) of the unrestrained model. This observation seems to indicate that the constraints we employed prevented the larger drift of the protein structure from the crystal structure.

The rms deviations were also determined for the nonhydrogen atoms of biotin. The rms deviation of the minimized structure was only 0.31 Å from the X-ray structure; the equilibrated structures deviated only 0.51 Å (no restraints) and 0.31 Å (H-bond restraints) from the X-ray structure.

Thirteen residues showed large displacements (> 2 Å) of their main chain atoms from the X-ray structure of the complex after the perturbation if the constraints were not employed. On the other hand, only the main chain atoms of Ala-46–Ala-50 and those of Ser-122 of the dyad-related subunit deviated in the same amount (> 2 Å) at $\lambda = 0$ in the case of the constrained simulation. Large deviations of Ala-46–Ala-50 correspond well to the crystallographic observation that the loop Ser-45–Ala-50 becomes ordered only after the binding of biotin. In some molecular dynamics studies on proteins and nucleic acids, restraints have been used to prevent deformations of the simulated structures from the X-ray structures.[41,42] This is due to the fact that the force field and the representation of the system (e. g., limited solvation of the macromolecules) is imperfect and the system has a tendency to drift from the experimental structure under these conditions unless constrained. The current system appears to fall in this category.

Concerning the constraint model, we carried out the perturbation in the reverse direction after 6 psec equilibration at $\lambda = 0$. Unfortunately, however, it was highly hysteretic as one can see in Table III. The system had drifted further from the X-ray and minimized structures as shown in Table IV although the deviations should be the same as those values of the equilibrated structure at $\lambda = 1$ in the ideal case. It was found that one water molecule remained in the binding pocket after the reverse perturbation ($\lambda = 1$). That water molecule was involved in the hydrogen bonds between biotin and streptavidin side chain atoms. This may be why the large hystereses in the free energy was observed. Given these structural "defects," we feel that the free energy change calculated for the reverse process is not an accurate measure of the binding free energy. Thus, ΔG_{prot} was calculated to be 24–36 kcal/mol from the forward simulations with the electrostatic and H-bonding energies of 14–20 kcal/mol and the VDW energy of 10–15 kcal/mol. It is appropriate to perform both forward and reverse perturbations to see the dependence of the free energy on starting structures and trajectories but in the case of the macromolecules reverse simulations are sometimes difficult[38] both because of drift from the initial crystal structure and because it may be harder for water molecules to come out of the binding pocket than for them to enter it. Thus, in this study, we have relied on different, independent simulations on the protein–ligand complex in the forward direction.

In the final structure ($\lambda = 0$) of the unrestrained

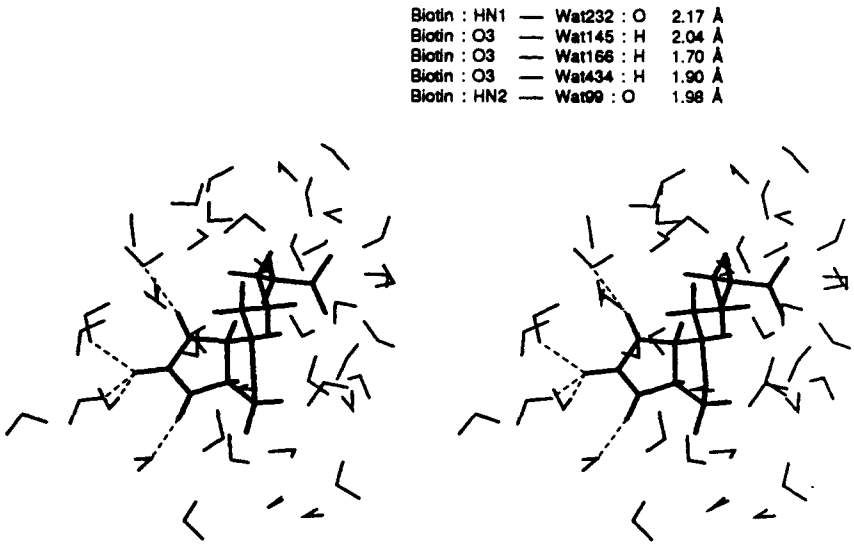

Fig. 4. Stereoviews of solvated biotin. The equilibrated structure with a residue-based nonbonded cutoff of 8 Å is given. Hydrogen bond distances between the ureido group of biotin and solvent are shown.

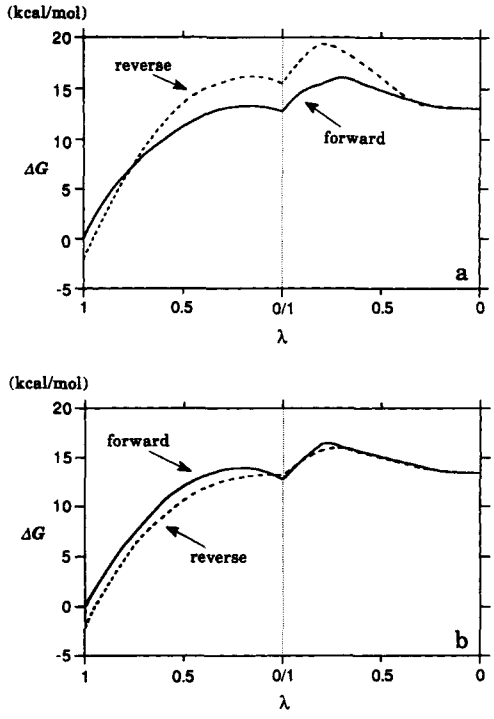

Fig. 5. Free energy changes versus λ for the perturbation biotin → partial dummy molecule (——) and its reverse, partial dummy molecule → biotin (– – –) in water. The left half corresponds to the electrostatic and H-bonding perturbation and the right half corresponds to the VDW mutation. (a) Run 2 in Table II. (b) Run 3 in Table II.

model, Trp-120 and Lys-121 showed large movements and two of water molecules came into the binding pocket to form hydrogen bonds with the protein side chains which were hydrogen bonded to the biotin ureido group in the initial state (λ = 1). In contrast, in the restrained model, one water molecule was found in the binding pocket without large movements of Trp-120 and Lys-121 (Fig. 6b). This structural difference might be related to the free energy difference between the restraint models.

The absolute binding free energy $\Delta G_{solv} - \Delta G_{prot}$ is calculated to be −21.0 and −9.4 kcal/mol for the simulations with and without restraints, respectively, as shown in Table V. Given this large range of values and the fact that we could not effectively run the reverse simulations in the protein, no detailed error estimates are given. Those values derived by the partial dummy molecule do not exactly correspond to the experimental ones because the perturbed molecule contains some real atoms. However, the contribution of the remaining $CH_2CH_2CH_2COO^-$ group to the absolute binding free energy (ΔG_0) is assumed to be relatively small since the carboxyl group of biotin is partially solvated even if biotin is bound to streptavidin. The calculated $\Delta\Delta G_{bind}$ of −21.0 to −9.4 kcal/mol seems to be in reasonable qualitative agreement with the experimental value of −18.3 kcal/mol.

The key result is that the VDW energy contribution (−15 to −9 kcal/mol) to the binding free energy dominates the electrostatic and H-bonding energy contribution (−6 to 0 kcal/mol). The calculations have clearly shown that although the electrostatic and H-bonding energies are larger than the VDW energy in the complex, similarly large energies of the electrostatic and H-bonding interactions are involved in solvation of the ligand. The comparable contributions of the electrostatic and H-bonding interactions to the free energy both in solvent and in

TABLE II. Free Energy Changes (ΔG_{solv}) for Perturbing Biotin Into a Partial Dummy Molecule in Aqueous Solution

		Simulation time* (psec)		ΔG_{solv}† (kcal/mol)		
Run	Program	Elec.‡	VDW§	Elec.	VDW	Total**
1	AMBER3A	30/30	30/30	9.8 ± 1.2	−0.7 ± 1.1	9.1 ± 2.2
2	AMBER4	30/30	30/30	15.1 ± 2.3	−1.1 ± 1.4	14.0 ± 1.1
3	AMBER4	30/30	48/56	14.1 ± 1.3	0.5 ± 0.3	14.5 ± 1.1

*Simulation times correspond to forward/reverse perturbations.
†Errors represent the half the hysteresis between forward ($\lambda = 1 \rightarrow 0$) and reverse ($\lambda = 0 \rightarrow 1$) simulations.
‡Electrostatic and H-bonding energies.
§VDW energy.
**Total interaction energy (elec. + vdw).

the protein are well understood because the H-bonding modes of the imidazolidone group of biotin are remarkably similar to each other as one can see in Figures 4 and 6a. Both in solution and in the protein, there are five hydrogen bonds between the ureido group and the surroundings, just as shown schematically in Figure 3.

Perturbation to the complete dummy molecule

In the mutation from biotin to the complete dummy molecule a residue-based nonbonded cutoff of 10 Å was used since the net atomic charge of the protein residues within 10 Å of the carboxyl moiety in the crystal structure was found to be zero. If the net charge changes during the perturbation, this charge neutrality of the protein is preferable because the corresponding charge of the water box is always equal to zero. In the free energy calculations the electrostatic decoupling option with the "slow growth" method was used. The electrostatic and volume changes are so large compared to the previous perturbation that simulation times were increased to 100 psec or more.

After the equilibration for 2 psec at 298 K with a nonbonded cutoff of 10 Å starting from the previously equilibrated structure which had been found using an 8 Å cutoff, the perturbation simulation of biotin in a water box was carried out, leading to a ΔG_{solv} of 93.8±2.1 kcal/mol without the Born correction, as shown in Table VI. The electrostatic free energy change was very large as expected and the VDW energy contribution was calculated to be −4.1±0.5 kcal/mol (i.e., unfavorable interactions of biotin with water), which was smaller than the corresponding value obtained for the partial dummy molecule by 4.6 kcal/mol. This difference is appropriate in light of the four methylene groups in the partial dummy molecule. The hystereses were a little larger than those found in the case of the partial dummy molecule but they seemed to be reasonable, given the larger size of the perturbation. After the perturbation of biotin to the dummy molecule, the topology of biotin was completely overlapped by water molecules and the box was of the correct density for pure water.

The geometry optimization of the solvated streptavidin–biotin complex with a nonbonded cutoff of 10 Å was carried out in two steps, trying to decrease the drift of the protein structure after the optimization. First, only water molecules were minimized with the protein held rigid. This was to prevent strong forces from the rearranging waters from disrupting the protein structure. The energy minimization was then performed on all the mobile residues. As one can see in Table IV, the resultant minimized protein structure was found to have slightly smaller deviations from the crystal structure than those of the minimized structure previously. No positional constraint on the ligand was applied since no real atom remained at the perturbed state.

The minimized system was equilibrated for 4 psec at 298K with the same internal restraints (2.8 Å, 25 kcal/mol·Å^2) on the five hydrogen bonds as before. An additional 2 psec equilibration without restraint was performed to obtain the starting structure of the unrestrained model. With respect to the restraint model, the restraints on the two hydrogen bonds between the carboxyl group of biotin and the protein residues were applied as well in order to imitate the similar fixing effect on the carboxyl terminal as that obtained by the positional constraint used in the mutation into the partial dummy molecule. Another 3 psec equilibration with the 5 kcal/mol·Å^2 restraint on seven hydrogen bonds was carried out based on the preequilibrated structure for 4 psec. The free energy simulations were done on these two equilibrated systems using the same protocol as before. At the last part of some of the VDW perturbations in the forward direction, the step size was lowered from 2 to 1 fsec because of SHAKE failures due, presumably, to large forces associated with disppearing atoms. The simulation in the reverse direction was not attempted this time.

Table VI shows the calculated free energy changes without Born corrections. The calculated values var-

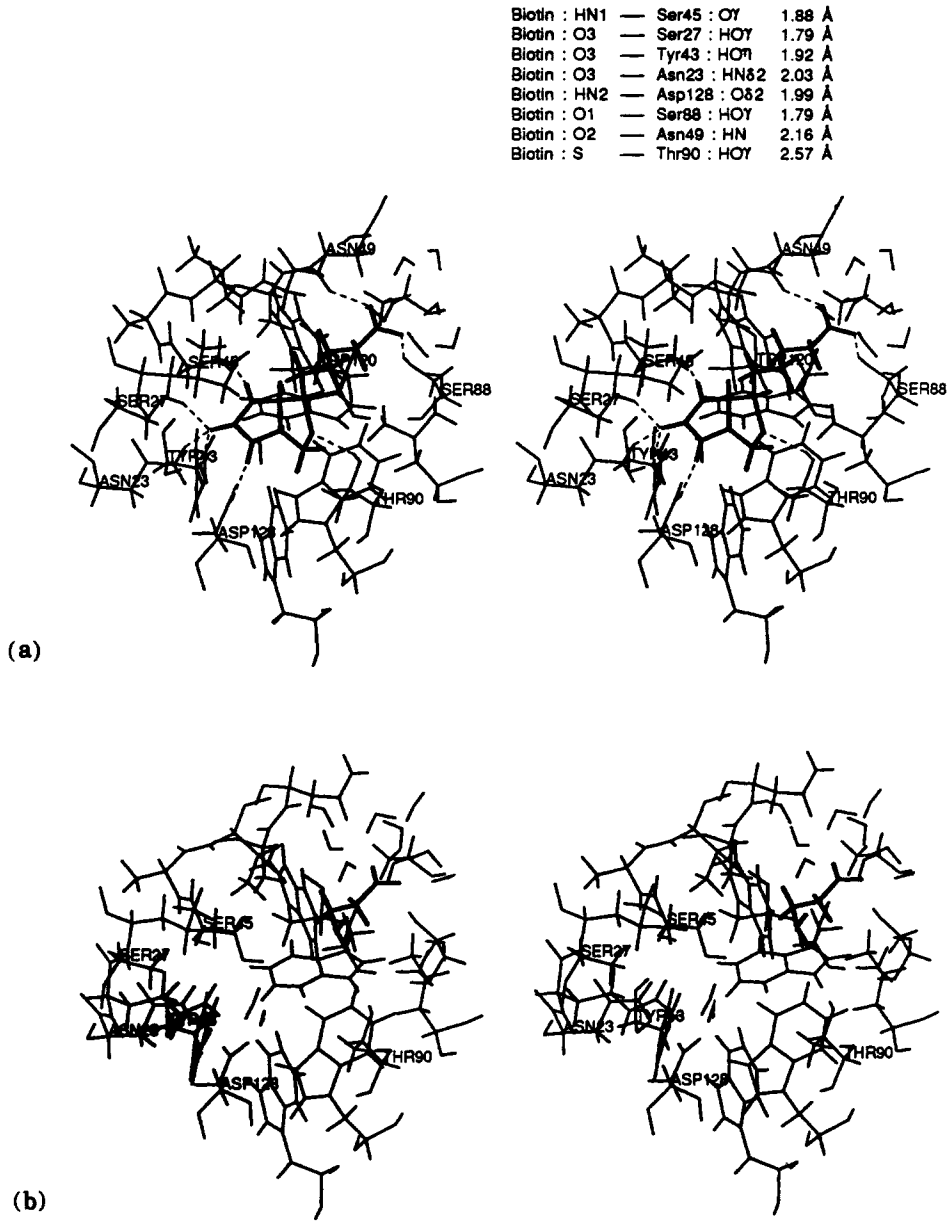

Fig. 6. Stereoviews of the binding site of the streptavidin–ligand complexes. Structures of the restraint model are given. (a) The equilibrated structure with biotin (λ = 1) using a nonbonded cutoff of 8 Å. Hydrogen bond distances between the ligand and the protein are shown. (b) The perturbed structure with the partial dummy molecule (λ = 0).

ied depending on the restraint models. Especially, the difference of the free energy changes based on the electrostatic and H-bonding interactions was significant. When the electrostatic and H-bonding free energy change (86.7 kcal/mol) of the unrestrained model was compared to that (97.9 kcal/mol) obtained in the solution simulation, a large positive value of 11.2 kcal/mol was found. It is unrealistic that the electrostatic and H-bonding interactions are so unfavorable in the protein compared to those in water. Examining the structure after the electrostatic perturbation, large positional changes of the side chain of Trp-120 and Lys-121 were found while those kinds of movements were observed only after the VDW perturbation in the other simulations. This conformational change was considered to be responsible for the energy artifact observed above.

In some studies relatively short simulation runs were used in order to obtain the trajectories that remained close to the X-ray structures as well as reliable free energies.[40b,42,43] Since rather long simulation times such as 100 psec were employed in the

TABLE III. Free Energy Changes (ΔG_{prot}) for Perturbing Biotin Into a Partial Dummy Molecule in Solvated Streptavidin

			Siml. time (psec)		ΔG_{prot} (kcal/mol)		
Run	Restraint*	Direction†	Elec.‡	VDW§	Elec.	VDW	Total**
1	No	Forward	36	48	14.4	9.5	23.9
2	Yes	Forward	36	48	20.3	15.2	35.5
3	Yes	Reverse	36	48	18.3	4.0	22.3

*Restraints on five hydrogen bonds between the uriedo group of biotin and streptavidin.
†Forward: $\lambda = 1 \rightarrow 0$; reverse: $\lambda = 0 \rightarrow 1$.
‡Electrostatic and H-bonding energies.
§VDW energy.
**Total interaction energy (elec. + vdw).

TABLE IV. Root Mean Square Deviations (Å) Between the Calculated Structures and Crystal, Minimized, and Equilibrated Structures*

		Crystal			Minimized			Equil.† ($\lambda = 1$)		
	Restraint	Main	Side	Total	Main	Side	Total	Main	Side	Total
Biotin→pDum‡										
Minimized		0.56	1.00	0.81						
Equil. ($\lambda = 1$)	No	0.70	1.26	1.01	0.61	0.94	0.79			
Forward ($\lambda = 0$)	No	0.94	1.89	1.49	0.90	1.65	1.33	0.86	1.43	1.17
Equil. ($\lambda = 1$)	Yes††	0.57	1.25	0.97	0.56	0.89	0.74			
Forward ($\lambda = 0$)	Yes††	0.72	1.46	1.15	0.78	1.26	1.05	0.69	1.19	0.97
Reverse ($\lambda = 1$)	Yes††	1.11	1.49	1.31	1.18	1.44	1.31	1.06	1.34	1.21
Biotin→cDum§										
Minimized		0.49	0.88	0.71						
Equil. ($\lambda = 1$)	No	0.67	1.21	0.98	0.60	0.93	0.78			
Forward** ($\lambda = 0$)	No	0.95	1.83	1.45	0.87	1.59	1.28	0.74	1.40	1.11
Equil. ($\lambda = 1$)	Yes‡‡	0.55	1.27	0.98	0.51	0.92	0.74			
Forward** ($\lambda = 0$)	Yes‡‡	0.76	1.76	1.35	0.76	1.46	1.16	0.71	1.41	1.11
Biotin→thiobiotin										
Forward ($\lambda = 0$)	No	0.88	1.76	1.39	0.83	1.43	1.16	0.74	1.26	1.03
Forward ($\lambda = 0$)	Yes§§	0.80	1.72	1.33	0.66	1.34	1.06	0.62	1.22	0.96
Reverse ($\lambda = 1$)	Yes§§	0.65	1.62	1.23	0.62	1.43	1.09	0.56	1.27	0.98
Biotin→iminobiotin										
Forward ($\lambda = 0$)	No	0.91	1.67	1.34	0.84	1.41	1.16	0.84	1.22	1.05
Forward ($\lambda = 0$)	Yes§§	0.80	1.43	1.15	0.74	1.19	0.99	0.73	1.01	0.92
Reverse ($\lambda = 1$)	Yes§§	0.87	1.64	1.31	0.82	1.37	1.13	0.72	1.23	1.01

*All deviations are calculated using the mobile nonhydrogen atoms of streptavidin.
†Equilibrated structure.
‡Partial dummy molecule.
§Complete dummy molecule.
**Short simulations of 30 psec (elec.) and 48 psec (vdw).
††Restraints on five hydrogen bonds including the ureido group of biotin.
‡‡Restraints on seven hydrogen bonds between biotin and streptavidin.
§§Restraints on two hydrogen bonds including the NH groups of biotin.

current case, we reran the calculation with the shorter simulation times used in the perturbation to the partial dummy molecule, which were still longer than those employed in the previous studies.[40b,42,43] These calculated values are also presented in Table VI. As one can see, the shorter simulations and the restraint model run with the long simulation times all yielded similar values. This indicates that the short simulation time is good/long enough to get a consistent free energy change in this system.

In the case of the unrestrained model, relatively small conformational changes of the side chains of Trp-120 and Lys-121 were observed after the perturbation. The VDW energy also changed considerably, probably because of the rather different initial structure for the VDW perturbation. Encouragingly, both free energy changes due to the electrostatic and H-bonding interactions and VDW interaction were found to be comparable for the two restraint models. The unrestrained model gave larger deviations of the structure than those of the restraint model, just as found in the case of the partial dummy molecule (Table IV).

Approximately six water molecules were observed

TABLE V. Comparison of Calculated Binding Energy ($\Delta\Delta G_{bind}$) of Biotin (→ Partial Dummy Molecule) With Experiment

		$\Delta\Delta G_{bind}$† (kcal/mol)		
Run	Restraint*	Elec.‡	VDW§	Total**
1	No	−0.3 ± 1.3	−9.0 ± 0.3	−9.4 ± 1.1
2	Yes	−6.2 ± 1.3	−14.7 ± 0.3	−21.0 ± 1.1
Experimental††				−18.3

*Restraints on five hydrogen bonds between the ureido group of biotin and streptavidin.
†Errors correspond to those obtained for the calculations of ΔG_{solv} (run 3 in Table II).
‡Electrostatic and H-bonding energies.
§VDW energy.
**Total interaction energy (elec. + vdw).
††Experimental data.[6b]

TABLE VI. Comparison of Calculated Binding Free Energy of Biotin (→ Complete Dummy Molecule) With Experiment

				Free energy changes (kcal/mol)‡		
	Restraint*	Siml. time† (psec)		Elec.§	VDW**	Total††
ΔG_{solv}		100/100	110/124	97.9 ± 1.6	−4.1 ± 0.5	93.8 ± 2.1
ΔG_{prot}	No	100	120	86.7	7.5	94.2
	No	36	48	99.0	15.0	114.0
	Yes	100	108	100.7	15.5	116.2
	Yes	36	48	101.0	14.0	115.0
$\Delta\Delta G_{bind}$	No	(36)	(48)	−1.1 ± 1.6	−19.1 ± 0.5	−20.2 ± 2.1
(calc.)	Yes‡‡	(100)	(108)	−2.8 ± 1.6	−19.6 ± 0.5	−22.4 ± 2.1
	Yes‡‡	(36)	(48)	−3.0 ± 1.6	−18.2 ± 0.5	−21.2 ± 2.1
$\Delta\Delta G_{bind}$	Exp.§§					−18.3

*Restraints on seven hydrogen bonds between biotin and streptavidin.
†Simulation time (forward/reverse). Values in parentheses correspond to those used for the calculation of ΔG_{prot}.
‡Errors, where listed, represent half the hysteresis between forward and reverse simulations in water.
§Electrostatic and H-bonding energies.
**VDW energy.
††Total interaction energy (elec. + vdw).
‡‡ΔG_{prot} of the restraint model were used for calculations of $\Delta\Delta G_{bind}$.
§§Experimental data.[6b]

in the binding pocket of both restraint models after the forward perturbation. One of the final mutated structures is shown in Figure 7. The number of the water molecules in the binding site may appear to be small to fill the space of vanishing biotin which has 16 heavy atoms. However, the cavities in proteins are not necessarily fully solvated as was shown by X-ray diffraction studies or theoretical techniques.[35,44] Interestingly, in the crystal structure of apostreptavidin (kindly provided to us by P. Weber), ~5–6 water molecules are found in the binding site cavity[3b] and Asp-128 carbosyl oxygens form hydrogen bonds with Asn-23HN$^{\delta 2}$, Trp-92HN$^{\epsilon 1}$ and a water molecule just outside the binding pocket. In the simulated structure (Fig. 7) also, Asp-128 was not hydrogen bonded to water molecules inside the cavity but hydrogen bonded to one outside, Asn-23HN$^{\delta 2}$, Gln-24HN$^{\epsilon 2}$, and Trp-108HN$^{\epsilon 1}$. Since all the positions of water molecules could not be determined by the X-ray analysis, there might be a frontally placed water molecule interacting with Asp-128 even in the crystal state, as was found in the perturbation to the partial dummy molecule (Fig. 6).

The free energy change due to the VDW interaction in the protein was larger in magnitude and opposite in sign to that for the corresponding perturbation in pure water and also showed a different dependence on λ. Figure 8 illustrates the free energy changes versus λ for the perturbation in water and in the protein. In the water system, the free energy increased with λ (1.0–0.67) and then decreased in the forward perturbation. In the protein, little change of the free energy was observed for the latter half after the large increase of the energy. In both cases the reduction of the well-depths and the radii of VDW parameters lead to the rise of the free energy, having the greatest variation in the initial perturbation region with the largest well-depths.

In solution the surrounding water molecules were able to collapse into the gap created by the vanishing perturbed ligand molecule. As the attractive interaction between the approaching waters became

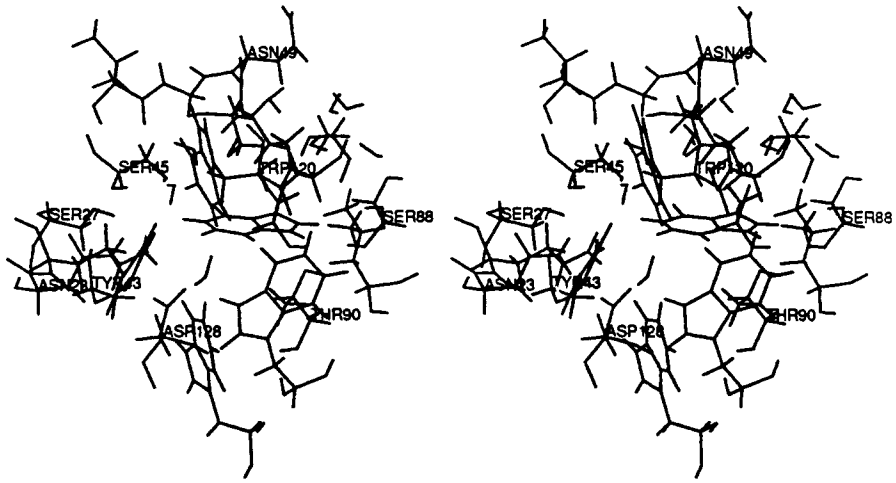

Fig. 7. Stereoviews of the binding site of the complex with streptavidin and the complete dummy molecule (not shown) ($\lambda = 0$). The perturbation was carried out using a residue-based nonbonded cutoff of 10 Å without restraints.

stronger, the repulsion between the ligand and water molecules dominates, resulting in the decline of the free energy. By contrast, this offset/decrease was not observed in the protein simulations because the protein residues were unable to reorder to fully occupy the cavity created by the disappearance of the ligand. As a result, the mutation of biotin into the complete dummy molecule in solution has a ΔG of ~ -4 kcal/mol (VDW interaction energy), due to the cancellation of dispersion and repulsion effects (Table VI). On the other hand, in the protein, a very small free energy price must be paid to create a cavity since one already exists. The VDW perturbation of biotin to the dummy molecule is energetically very unfavorable with the ΔG of $\sim$ 15 kcal/mol, because of the loss of attactive VDW interactions.

A 6-31G* basis set used for the calculation of the partial charges of the ligand leads to dipole moments larger than experiment typically by 10–20%,[45] comparable to the enhancement of the water dipole in the TIP3P water model.[30] Thus, the electrostatic charges in the water box are likely to be well-balanced. On the other hand, the partial atomic charges of the protein residues were derived[25] based on a STO-3G basis set which does not produce the dipole exaggeration, resulting in the possible imbalance of the polarization between the ligand and the protein. The free energy dependence on the electrostatic charge, therefore, needed to be investigated.

The perturbations of the partial atomic charges of biotin were performed both in water and in the protein; the electrostatic charges derived by the 6-31G* basis set were mutated into those calculated with the STO-3G basis set. The free energy changes were calculated to be 16.0±0.1 kcal/mol for the perturbation in water from the 30 psec simulations. The corresponding values of 16.4±0.7 and 14.7±0.1 in the protein were obtained with and without restraints, respectively, from the 30 psec simulations in both directions. The comparable free energy differences indicate that the above calculated $\Delta\Delta G_{bind}$ for the absolute binding free energy is relatively independent of the atomic charges, while the absolute free energy due to the electrostatic interaction is found to be much smaller in the case of the partial charges derived by the STO-3G basis set. This result also suggests that the atomic partial charges of the TIP3P water model and the protein residues may be adequately balanced with respect to the FEP calculations.

The Born corrections for the free energy changes of the perturbations both in water and in the protein might be expected to be similar since the same value of the nonbonded cutoff was used in both cases, although the cancellation would not be exact because periodic boundary conditions were applied only to the simulations in the water box. Since it is likely that the difference in the Born corrections is small and because these conditions are difficult to accurately estimate, we assume complete cancellation of the Born corrections. Thus, from the short simulations, the absolute binding free energy $\Delta G_{solv} - \Delta G_{prot}$ was then calculated to be -21.2 and -20.2 kcal/mol for the models with and without restraints, respectively, as shown in Table VI. In the long simulation with restraints the absolute binding free energy was calculated to be -22.4 kcal/mole.

Relative Binding Free Energy Calculations

The calculations of the relative binding free energies were carried out by mutating biotin to thiobiotin and iminobiotin both in water and in streptavidin with a nonbonded cutoff of 8 Å. The perturbation calculations were performed based on the same

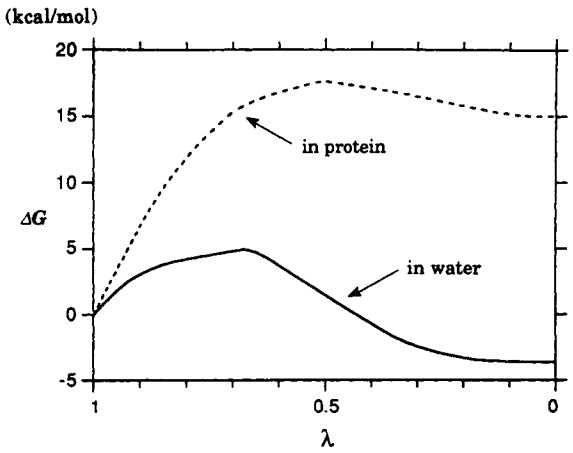

Fig. 8. Free energy changes due to the VDW perturbation versus λ for the biotin → complete dummy molecule mutation in aqueous solution (——) and in the solvated protein (– – –). The free energy change for the protein simulation represents that of the unrestrained model with shorter simulation time.

equilibrated structures as those used in the perturbation to the partial dummy molecule. Since the perturbed moieties were rather small, shorter simulation time of 40 psec in each direction was applied without the electrostatic decoupling option. In the simulations of the protein–ligand complexes, two kinds of internal distance restraint models were examined without positional constraints on the ligand. In one model the restraints were applied to the two hydrogen bonds including each of the ureido NH of biotin. No restraint was used in the other model.

In the perturbation from biotin to thiobiotin in the solvated protein, three hydrogen bonds between the oxygen atom and the protein residues were found to be changed into four weaker hydrogen bonds between the mutated sulfur atom and the same protein residues with the average distances of 3.3 and 3.4 Å for the restraint and unrestrained models, respectively. Figure 9 illustrates the perturbed structure (λ = 0) of the restraint model. The hydrogen bond to the NH group of the Asn-23 side chain was mutated into two hydrogen bonds between the sulfur atom and both of the hydrogens of the Asn-23 NH_2 group. These observations correspond well to the large VDW radius and weak H-bonding nature of a sulfur atom.

The simulation of the unrestrained model in the reverse direction was not attempted since both hydrogen bonds concerning to the ureido NH group were almost broken (3.7 and 4.0 Å) after the forward simulation. Similar to the perturbation to the dummy molecules, the restraint model yielded smaller deviations than those of the unrestrained model as shown in Table IV. The rms deviations of the biotin complex after the reverse simulation were slightly reduced compared to those of the thiobiotin complex in the restraint model while one hydrogen bond involving the carbonyl oxygen of biotin was somewhat broken (3.6 Å) in the reverse structure. Thus, it appears that the perturbation of the structure carried out for thiobiotin is partially reversible.

As for the binding of iminobiotin, experimental results showed that only the free base form of iminiobiotin was firmly bound by avidin although the pK_a of the guanidino group of iminobiotin was found to be 11.9. The binding free energy (−14.3 kcal/mol) of this form was calculated from the observed dissociation constant at a lower pH, using the measured pK_a of the guanidino moiety.[6] There are geometric isomers with respect to the hydrogen configuration of the guanidino group. In order to presume the probable isomer of these bound to the protein, the complexes of both isomers were model built and energy minimized. Since the isomer shown in Figure 2 was found to give a more stable complex by 9.7 kcal/mol than the other, it was used throughout the following simulations.

In the mutation from biotin to iminobiotin in the complex, two of the three hydrogen bonds involving the carbonyl oxygen of the ureido group were preserved, changing into the corresponding hydrogen bonds between the mutated nitrogen atom of the guanidino group and the protein (Fig. 10). The other hydrogen bond between the ureido oxygen and Asn-23$HN^{\delta 2}$ was found to be replaced by two weak hydrogen bonds consisting of the mutated nitrogen atom and Asn-23$HN^{\delta 2}$ (~3.3 Å), and the hydrogen of the mutated NH and Asp-128$O^{\delta 2}$ (~3.6 Å). Therefore, the total H-bonding interactions were considered to be comparable between biotin and iminobiotin. On the other hand, stronger hydrogen bonds were formed if the iminobiotin was fully solvated as shown in Figure 11, which was obtained through the perturbation of biotin into iminobiotin in water. The comparison of the H-bonding modes of the ligands in solution also suggests that the solvation energy of iminobiotin is expected to be larger than that of biotin.

The reverse direction perturbation of the nonconstrained model was not carried out because the hydrogen bond between the NH group of the guanidino moiety and Ser-45O^{γ} was broken (5.7 Å) in the forward simulation. The reduction of the rms deviation of the biotin complex after the reverse simulation with the restraint model was not observed while all of the three hydrogen bonds involving the carbonyl oxygen of the biotin were successfully formed in the final structure. From the structural point of view, our simulations predict the structures of the streptavidin complexes with thiobiotin and iminobiotin as described above.

Table VII summarizes the calculated and experimental free energy changes. The hystereses are small and the free energy differences among the restraint models of the complex systems are similar to or smaller than those in the calculations of the abso-

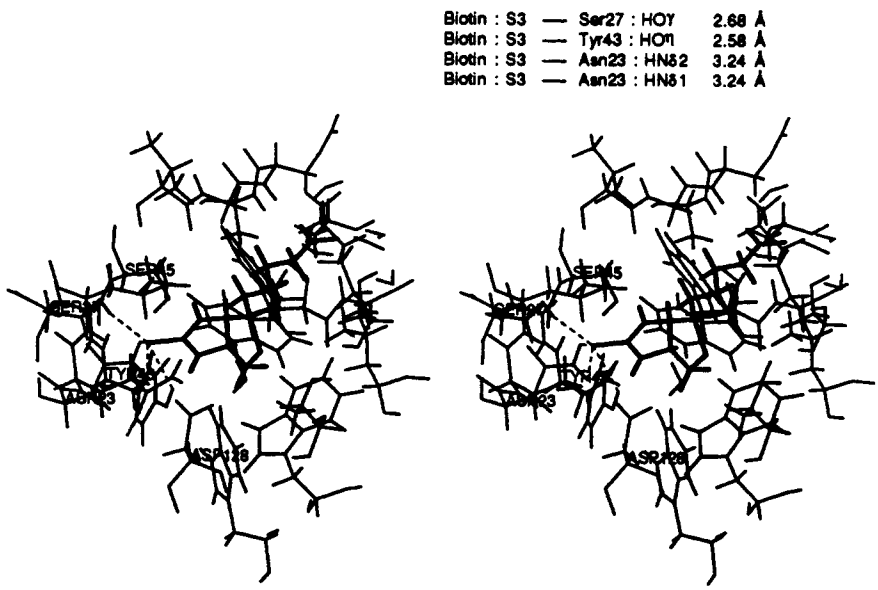

Fig. 9. Stereoviews of the binding site of the streptavidin–thiobiotin complex. The perturbed structure (λ = 0) of the restraint model is given. Hydrogen bond distances between the ligand and the protein are shown.

lute binding free energy. This is probably due to the smaller mutations and the short simulation time. As is suggested by the comparison of the H-bonding mode of the ligands, ΔG_{solv} obtained for the mutation of biotin into iminobiotin is a negative value of −5.3 kcal/mol, showing the stronger interactions between iminobiotin and water. In contrast, the relative solvation free energy of biotin and thiobiotin is calculated to be 8.8 kcal/mol, consistent with the weaker H-bonding nature of the sulfur atom. The calculated relative free energies ($\Delta\Delta G = \Delta G_{bind2} - \Delta G_{bind1}$) of 3.2 and 4.4 kcal/mol and 6.5 and 7.8 kcal/mol for binding to streptavidin are in nearly quantitative agreement with the experimental values of 3.6 and 6.2 kcal/mol, respectively, determined from binding of biotin and its two analogs to avidin. This level of agreement strongly supports the conservation of the essential features of the binding pockets of avidin and streptavidin and is excellent in the case of the mutation into thiobiotin.

DISCUSSION

The calculated absolute binding free energies of biotin to streptavidin of −20.2 to −22.4 kcal/mol with the three most reliable models presented above are in reasonable agreement with experimental value of −18.3 kcal/mol. Considering the large perturbation carried out, the agreement is impressive. To our knowledge this is among the first successful computational studies of the absolute binding free energy of complexation of a protein and a ligand and is particularly important because the biotin–avidin complex is one of the strongest known protein–ligand associations. The results of our study are also significant because the VDW interactions play a more important role than the electrostatic and H-bonding interactions in ligand binding. This is a profound and interesting result and, as noted above, comes from the hydrophobic effect, which makes the ΔG of VDW interactions in solution so small. The present study gives clear insight into the binding nature of the streptavidin–biotin complex, showing the significant contribution of the hydrophobic interactions to the free energy of binding.

Weber et al. suggested that the ureido group is unusually polarizable and that significant $C^{\delta+}$–$O^{\delta-}$ character in this system is suggested by the three proton donors to this group in the protein.[3] It is not clear how important this effect is in energy terms, since the same hydrogen bond pattern is found in solution (Fig. 4). It is also possible that the ureido C=O prefers out of plane donors because these orientations lead to less repulsive "secondary interactions"[46] than in plane approaches. In addition, our interpretation also helps explain the results recently presented by Weber et al.[3b] They found that HABA, a benzoic acid derivative with its negative CO^{2-} replacing the ureido $C^{\delta+}$–$O^{\delta-}$ of biotin bound to streptavidin with a free energy of association of only −5.3 kcal/mol, despite the preservation of key hydrogen bond interactions with protein residues. This is completely consistent with our interpretation that VDW effects rather than electrostatic provide the dominant stabilization of the biotin–streptavidin complex.

It helps, in the case of streptavidin, to have four tryptophan ligands to increase the favorable dispersion attraction. One hundred and twenty-eight at-

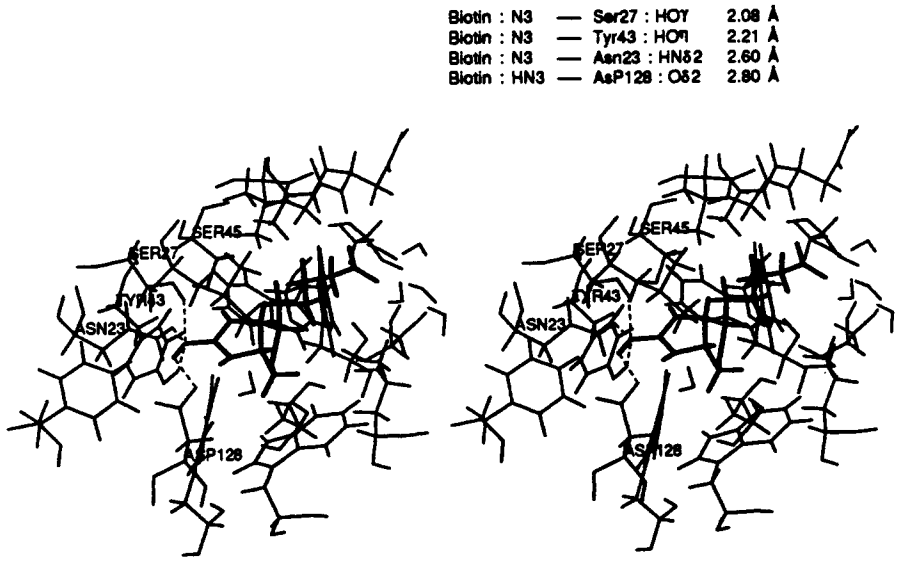

Fig. 10. Stereoviews of the binding site of the streptavidin–iminobiotin complex. The perturbed structure ($\lambda = 0$) of the restraint model is given. Hydrogen bond distances between the ligand and the protein are shown.

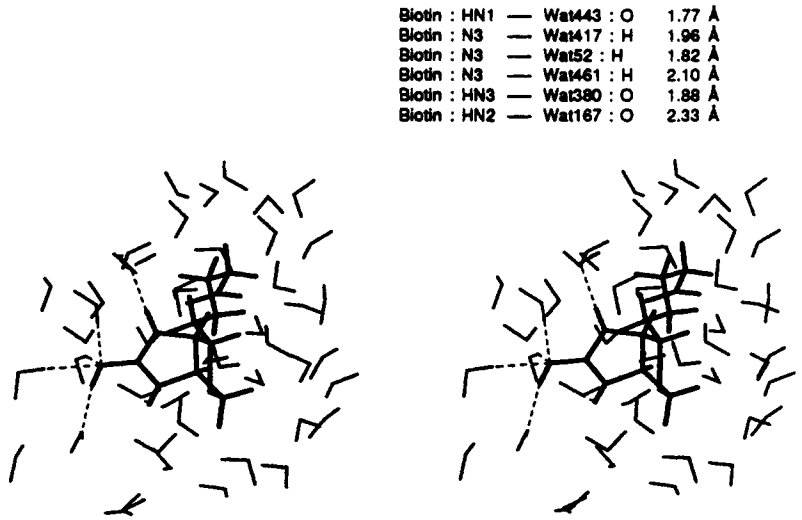

Fig. 11. Stereoviews of solvated iminobiotin. The perturbed structure from biotin with a nonbonded cutoff of 8 Å is given. Hydrogen bond distances between iminobiotin and solvent are shown.

oms of streptavidin have short contacts (< 4 Å) to biotin. Although we have not quantitated the free energy contribution due to each residue in the binding site, based on the number of van der Waals contacts, Trp-79 and Trp-108 would be expected to contribute the most to the protein·ligand binding. It will be interesting to carry out site specific mutagenesis of these Trp residues as well as those (Asn-23, Ser-27, and Tyr-43) of the ureido hydrogen bonding triad.

As discussed above there were somewhat contradictory experimental data on the nature of the binding. The calculated results support the postulated interpretation that the entropy increase to be expected from hydrophobic interactions is counterbalanced by a decrease in entropy accompanying the formation of buried hydrogen bonds.[6] The simulations indicate that the free energy contribution of the hydrogen bonds between the ureido group of biotin and the protein is large in the complex but that the similar contribution of the ureido group hydrogen bonds also exists in the water solvent. The current results suggest that the ureido group provides a specific but weak anchoring point and that ex-

TABLE VII. Results of Relative Free Energy Calculations* (kcal/mol)

Perturbation	Restraint†	ΔG_{solv}	ΔG_{prot}	$\Delta\Delta G_{bind}$ Calc. $\Delta G_{prot} - \Delta G_{solv}$	$\Delta\Delta G_{bind}$ Exp.‡ $\Delta G_{bind2} - \Delta G_{bind1}$
Biotin→ thiobiotin	No	8.8 ± 0.1	13.2§	4.4 ± 0.1	3.6
	Yes		12.0 ± 0.3	3.2 ± 0.3	3.6
Biotin→ iminobiotin	No	−5.3 ± 0.1	2.5§	7.8 ± 0.1	6.2
	Yes		1.2 ± 0.7	6.5 ± 0.8	6.2

*Errors, where listed, correspond to the half the hysteresis between forward and reverse runs.
†Restraints on two hydrogen bonds between the NH groups of biotin and streptavidin.
‡Experimental data.[6a]
§Calculation only from forward perturbation.

tensive hydrophobic interactions lead to the great stability of binding, as was inferred by Green.[8] Entropy–enthalpy compensation and the large temperature dependence of each of them make the sign and magnitude of the entropy and enthalpy a poor predictor of the hydrophobic effect; thus, it would be of interest to determine the ΔC_p associated with the biotin–avidin association and the site specific mutagenesis of Trp-79 and Trp-108.

Given the surprisingly good agreement between the calculated and observed absolute ΔG of binding, let us examine critically whether this agreement is fortuituous or lucky. Clearly, there are a number of significant approximations inherent in the way the calculations were done. The approximations can be divided into the two general difficulties inherent in any molecular dynamics/Monte Carlo simulation on a macromolecule: (1) sampling and (2) force field.

Under "sampling" come four issues: (a) first, starting with the biotin–streptavidin complex, (1) How well do our calculations represent the structural nature of the protein in the uncomplexed state? (2) How well do the calculations represent active site hydration in the uncomplexed state? (3) What are the free energy consequences of constraining the hydrogen bond distances of biotin–streptavidin as it disappears? and (d) What is the consequence of not including the intramolecular free energies of biotin in both protein and solution?

Although we cannot claim to have accurately modeled the unbound state of streptavidin as biotin "disappears," it is encouraging that the parts of the streptavidin that move most during complexation, the flexible loop between residues 45–50, also have moved significantly as biotin is mutated to nothing. In any case, representing any such conformational change inadequately would be expected to lead to a ΔG_{prot} too large in magnitude since the uncomplexed state would be calculated to be higher in free energy than it should be.

As biotin disappears, what fills the space it leaves behind? In the "disappearance" of biotin in solution, carrying out the free energy calculations at constant pressure smoothly allows water to replace biotin as it disappears. The situation is more complex in the binding site of the protein with "capped" waters applied with half-harmonic radial forces. Our simulations suggest there are ~ 6 waters in the binding site cavity. Surprisingly, there was no "frontal" water H-bonding to Asp-128. One might imagine that the free energy consequence of not having a water in that position would be significant. To be sure, in this state ($\lambda = 0$), the Asp-128 CO_2^- is stabilized by a number of hydrogen bonds as described above. Interestingly, in the crystal structure of uncomplexed biotin, the closest water frontally placed (along the CO_2^- bisector) is 4.46 Å from the nearest oxygen. Thus, there may be a water there, but it does not seem to be strongly held.

More significantly, the free energy consequences of an incorrectly hydrated active site is difficult to quantitate. It is probably unfavorable to leave hydrophilic groups dehydrated, but favorable to leave hydrophobic groups unhydrated. Wade et al. have analyzed the free energies of waters in cavities in proteins and found that the free energy change for binding a water in a protein cavity (relative to keeping it in solution) can be small and of either sign.[35] Again, we cannot claim that we have an ideally hydrated active site cavity, but any error we make in this will raise the free energy of the uncomplexed state.

Third, in our perturbation simulations in the protein, especially in the case of the restrained models, the free energy change due to the loss of translational and rotational entropy in molecular association might be somewhat underestimated because of the restricted motion of the ligand in the binding pocket. This has been rigorously evaluated for the equilibrium between Xe gas and its binding to myoglobin.[15] Unfortunately, there seems to be no definitive method to compute an effective correction for the above factor for polyatomic molecules although the changes in translational/rotational entropy were estimated for the simple dimerization of urea in aqueous solution by Doig et al.[47] D. Williams (personal communication) suggests that the total of such a $T\Delta S$ term will be in the range of 2–7 kcal/mol and

as noted, it is hard to estimate how much of this total applies to our system. In the present study, therefore, no correction for the possible entropy loss is applied and further research will be necessary in order to calculate this kind of correction accurately. In any case, such an error will tend to overestimate the free energy of the uncomplexed state.

Finally, the neglect of intramolecular free energies for biotin will also lead to an overestimate of the free energy of the uncomplexed state. This comes mainly from the fact that the $(CH_2)_4$ CO_2^- side chain of biotin will have only one or a few low energy conformations when bound to steptavidin, but many low energy conformations when free in solution. What is the likely magnitude of this effect? If the unbound state has 10–100 times the number of allowed (low energy) conformations as the bound state (the maximum number allowed conformations for the unbound state is $\sim 3^4$, since there are 4 C–C bonds in the flexible side chain that can have g^+, g^-, or t conformations), this would correspond to a free energy of stabilization of the uncomplexed state of 1.4–2.8 kcal/mol.

In summary, all the four above-mentioned sampling limitations will lead to a calculated overestimate of the magnitude of ΔG_{prot}. On the other hand, the sign of the error in the calculated ΔG due to imperfect force field is harder to establish, but likely errors could come from the electrostatic parameters used. However, by mutating the STO-3G charges, which underestimate polarity, to 6-31G* charges, which overestimate it, we have shown that the calculated $\Delta\Delta G_{bind}$ does not appear to be very sensitive to the charges used. Nonetheless, it is still possible that nonadditive polarization effects emphasized by Weber et al.[3] are large, although, as argued above, we expect these to be similar in solution and in the protein. We cannot rule out that polarization effects will increase the calculated ΔG_{prot} and then one would have to invoke large errors in the ΔG due to sampling to bring it nearer to experiment. Arguing against this is the success we and others[15–19] have recently had in calculating absolute free energies for protein–ligand complexes. We studied[48] *N*-acethyltryptophanamide binding to α-chymotrypsin using exactly the same protocol as here and achieved reasonable calculated ΔG values, larger in magnitude than found experimentally by almost the same amount (~2–4 kcal/mol) as we have found in biotin–streptavidin. Thus, our approach seems powerful and general. It may not work in every case, but it is certainly promising.

As computer power grows, we will be able to study the biotin–streptavidin dissociation with PMF methods. It is well known that one can calculate the free energy as a function of coordinate or potential of mean force (PMF).[18] Although the FEP method based on Scheme I was used in the above calculations, the PMF calculation also allows one to determine the binding free energy by integrating the PMF curve over all coordinates. These simulations are typically much more time consuming and more complex than the FEP simulations. Therefore, the opportunity to make direct and meaningful comparison with experimental free energies of association has been limited to a few cases.[46b,49] In any case, the free energy determined by integrating the PMF curve is typically higher than the free energy at the minimum in the curve.[49b] In Scheme I, we are only sampling the minimum and infinitely separated points on the PMF curve.

The understanding of solvation and desolvation of ligands is critical as well as that of stabilization energies if the intermolecular interactions of ligands with proteins are to be described.[40,50] The relative free energy calculations have shown that biotin interacts more strongly with the protein than thiobiotin by about 13 kcal/mol while it is more difficult to desolvate biotin than thiobiotin by 8.8 kcal/mol (Table VII). This is why biotin is a better ligand of streptavidin than thiobiotin. In contrast to thiobiotin, the interaction energy of iminobiotin with the protein is smaller than that of biotin by only about 2 kcal/mol although it requires 5.3 kcal/mol more free energy to desolvate iminobiotin than biotin, placing iminobiotin as a weaker binding ligand than thiobiotin. This energy difference is probably due to the stronger hydrogen bonds formed by iminobiotin in water compared to those found in the protein. The results certainly show that the solvation energy (ΔG_{solv}) plays an important role in determining the relative binding affinity of these ligands. The agreement with the relative binding data for biotin analogs binding to avidin is particularly noteworthy, since the calculations were done on streptavidin rather than avidin. The absolute affinity of biotin is 2 kcal/mol smaller for streptavidin than avidin, but our calculations suggest the relative affinities of analogs will be better preserved.

CONCLUSIONS

We have shown that the molecular dynamics/FEP method can be successfully applied to study the binding affinity of biotin and its analogs with streptavidin. In the case of the absolute binding free energy calculations, the simulations are able to qualitatively reproduce the experimental binding free energy, although for long simulations restraints are necessary in order to compensate for the imperfection of the model system. Our study is among the first to calculate the absolute binding free energy of complexation of a protein and a complex ligand; encouragingly, we find that the calculated free energies with our three most reliable models ($\Delta G = -20$ to -22 kcal/mol) to be in reasonable agreement with the experimental ΔG of -18 kcal/mol. The calculated results give clear insights into the binding nature of the protein–ligand complex, showing that the

VDW/hydrophobic interaction energy dominates over the electrostatic and H-bonding energies in the binding of biotin by streptavidin.

The agreement with experiment is also near quantitative with respect to the relative binding free energy calculations between biotin, thiobiotin, and iminobiotin. Desolvation of the ligand is found to be important in understanding the relative affinity of ligands with proteins. Overall, the simulations presented here have "stretched the boundaries" for successful and useful applications of FEP calculations in protein–ligand systems, although improvement in force fields and more complete environmental representations are subjects of future research. Importantly, we have shown that using a theoretical method, it is currently possible to increase our understanding of the energetic factors affecting the binding interactions of protein–ligand complexes.

ACKNOWLEDGMENTS

We thank Dr. P. C. Weber for providing us with the crystal coordinates of the streptavidin–biotin complex and of streptavidin alone and Dr. C. I. Bayly for valuable discussions. The use of the facilities of the UCSF Computer Graphics Lab (R. Langridge, P. I., supported by NIH-RR-1081) and the San Diego Supercomputer Center for computer time are also gratefully acknowledged. PAK is grateful for research support from the NIH (GM-29072).

REFERENCES

1. Green, N. M. Avidin. Adv. Protein Chem. 29:85–143, 1975.
2. (a) Buckland, R. M. Strong signals from streptavidin-biotin. Nature (London) 320:557–558, 1986; (b) Bayer, E. A., Wilchek, M. The use of the avidin-biotin complex as a tool in molecular biology. Methods Biochem. Anal. 26:1–45, 1980; (c) Fucillo, D. A. Application of the avidin-biotin technique in microbiology. Biotechniques 3:494–501, 1985.
3. (a) Weber, P. C., Ohlendorf, J. J., Salemme, F. R. Structural origins of high-affinity biotin binding to streptavidin. Science 243:85–88, 1989, (b) Weber, P. C., Wendoloski, J.J., Pantoliano, M.W., Salemme, F.R. Crystallographic and thermodynamic comparison of natural and synthetic ligands bound to streptavidin. J. Am. Chem. Soc. 114:3197–3200, 1992.
4. Chaiet, L., Wolf, F. J. The properties of streptavidin, a biotin-binding protein produced by Steptomycetes. Arch. Biochem. Biophys. 106:1–5, 1964.
5. Argaraña, C. E., Kuntz, I. D., Birken, S., Axel, R., Cantor, C. R. Molecular cloning and nucleotide sequence of the steptavidin gene. Nucleic Acids Res. 14:1871–1882, 1986.
6. (a) Green, N. M. Thermodynamics of the binding of biotin and some analogues by avidin. Biochem. J. 101:774–780, 1966; (b) Green, N. M. Avidin and steptavidin. Methods Enzymol. 184:51–67, 1990.
7. Green, N. M. Avidin. 3. The nature of the biotin binding site. Biochem. J. 89:599–609, 1963.
8. Kauzmann, W. Some factors in the interpretation of protein denaturation. Adv. Protein Chem. 14:1–64, 1959.
9. Postma, J., Berendsen, H., Haak, J. Thermodynamics of cavity formation in water. A molecular dynamics study. Faraday Symp. Chem. Soc. 17:55–67, 1982.
10. (a) Warshel, A. Dynamics of reactions in polar solvents. Semiclassical trajectory studies of electron transfer and proton transfer reactions. J. Phys. Chem. 86:2218–2224, 1982; (b) Warshel, A. Dynamics of enzymatic reactions. Proc. Natl. Acad. Sci. U.S.A. 81:444–448, 1984. (c) Tembe, B. L., McCammon, J. A. Ligand receptor interactions. Comput. Chem. 8:281–283, 1984.
11. Singh, U. C., Brown, F. K., Bash, P. A., Kollman, P. A. An approach to the application of free energy perturbation methods using molecular dynamics. J. Am. Chem. Soc. 109:1607–1614, 1987.
12. (a) Bash, P. A., Singh, U. C., Brown, F. K., Langridge, R., Kollman, P. A. Calculation of the relative change in binding free energy of a protein-inhibitor complex. Science 235: 574–576, 1987; (b) Bash, P. A., Singh, U. C., Langridge, R., Kollman, P. A. Free energy calculations by computer simulation. Science 236:564–568, 1987.
13. Rao, S., Bash, P. A., Singh, U. C., Kollman, P. A. Free energy perturbation calculations on binding and catalysis after mutating Asn 155 in subtilisin. Nature (London) 328: 551–554, 1987.
14. (a) van Gunsteren, W. F. The role of computer simulation techniques in protein engineering. Protein Eng 2:5–13, 1988; (b) Brooks, C. L., III, Karplus, M., Pettitt, B. M. Proteins: A theoretical perspective of dynamics, structure and thermodynamics. Adv. Chem. Phys. 79, 1988; (c) Beveridge, D. L., DiCapua, F. M. Free energy via molecular simulation application to chemical and biomolecular systems. Annu. Rev. Biophys. Biophys. Chem. 18:431–492, 1989.
15. Hermans, J., Shankar, S. The free energy of xenon binding to myoglobin from molecular dynamics simulations. Isr. J. Chem. 27:225–227, 1985.
16. Merz, K. M., Jr. CO_2 binding to human carbonic anhydrase II. J. Am. Chem. Soc. 113:406–411, 1991.
17. Lee, F. S., Chu, J-T, Bolger, M. B., Warshel, A. Calculations of antibody-antigen interactions: Microscopic and semi-microscopic evaluation of the free energies of binding of phosphorylcgoline analogs to McPC603. Protein Eng. 5:215–228, 1992.
18. Jorgensen, W. L., Buckner, J. K., Boudon, S., Tirado-Rives, J. Efficient computation of absolute free energies of binding by computer simulations. Application to methane dimer in water J. Chem. Phys. 89:3742–3746, 1988.
19. Miyamoto, S., Kollman, P. A. Molecular dynamics studies of calixspherand complexes with alkali metal cations: Calculation of the absolute and relative binding of cations to a calixspherand. J. Am. Chem. Soc. 114:3668–2674, 1992.
20. (a) Singh, U. C., Weiner, P. K., Caldwell, J., Kollman, P. A. AMBER 3.0, University of California, San Francisco, California 1986; (b) Seibel, G., Singh, U. C., Weiner, P. K., Caldwell, J., Kollman, P. A. AMBER 3.0, Revision A, University of California, San Francisco, California 1989; (c) Pearlman, D. A., Case, D. A., Caldwell, J., Seibel, G., Singh, U. C., Weiner, P. K., Kollman, P. A. AMBER 4.0, University of California, San Francisco, California, 1990.
21. Jorgensen, W., Ravimohan, C. Monte Carlo simulation of differences in free energies of hydration. J. Chem. Phys. 83:3050–3054, 1985.
22. (a) Beveridge, D. L., Schnuelle, G. W. Free energy of a charge distribution in concentric dielectric continua. J. Phys. Chem. 79:2562–2566, 1975; (b) Aue, D. H., Webb, H. M., Bowers, M. T. A thermodynamic analysis of solvation effects on the basicities of alkylamines. An electrostatic analysis of substituent effects. J. Am. Chem. Soc. 98:318–329, 1976.
23. Berendsen, H. J. C., Postma, J. P. M., van Gunsteren, W. F., DiNola, A., Haak, J. R. Molecular dynamics with coupling to an external bath. J. Chem. Phys. 81:3684–3690, 1984.
24. Åqvist, J. Ion-water interaction potentials derived from free energy perturbation simulations. J. Phys. Chem. 94: 8021–8024, 1990.
25. (a) Weiner, S. J., Kollman, P. A., Case, D. A., Singh, U. C., Ghio, C., Alagona, G., Profeta, S., Jr., Weiner, P. A new force field for molecular mechanical simulation of nucleic acids and proteins. J. Am. Chem. Soc. 106:765–784, 1984; (b) Weiner, S. J., Kollman, P. A., Nguyen, D. T., Case, D. A. An all atom force field for simulations of proteins and nucleic acids. J. Comput. Chem. 7:230–252, 1986.
26. (a) Mak, T. C. W. Jasim, K. S., Chieh, C. Spectroscopic and structural studies of some bisdithiocarbamates and cyclic thiones. Can. J. Chem. 62:808–813, 1984; (b) Battaglia, L. P., Corradi, A. B., Nardelli, M. Structural aspects of 2-thioimidazolidine coordination in silver (I) halide complexes.

Croat. Chem. Acta 57:545–563, 1984; (c) Martin, M. L., Filleux-Blanchard, M. L., Martin, G. J., Webb, G. A. Application of nitrogen-15 spectroscopy and dynamic NMR to the study of ureas, thioureas and their Lewis acid adducts. Org. Magn. Reson. 13:396–402, 1980; (d) Stewart, W. E., Siddall, III T. H. Nuclear magnetic resonance studies of amides. Chem. Rev. 70:517–550, 1970.

27. Jorgensen, W. L., Tirado-Rives, J. The OPLS potential function for proteins. energy minimizations for crystals of cyclic peptides and crambin. J. Am. Chem. Soc. 110:1656–1666, 1988.
28. Singh, U. C., Kollman, P. A. An approach to computing electrostatic charges for molecules. J. Comput. Chem. 5:129–145, 1984.
29. GAUSSIAN 80 UCSF: Singh, U. C., Kollman, P. A. QCPE 2:17, 1982.
30. Jorgensen, W. L., Chandrasekhar, J., Madura, J. D., Impey, R. W., Klein, M. L. Comparison of simple potential functions for simulating liquid water. J. Chem. Phys. 79: 926–935, 1983.
31. (a) van Gunsteren, W. F., Berendsen, H. J. C. Algorithms for macromolecular dynamics and constraint dynamics. Mol. Phys. 34:1311–1327, 1977; (b) Ryckaert, J. P., Ciccotti, G., Berendsen, H. J. C. Numerical integration of the cartesian equations of motion of a system with constraints: Molecular dynamics of n-alkanes. J. Comput. Phys. 23: 327–341, 1977.
32. Pearlman, D. A., Kollman, P. A. A new model for carrying out free energy perturbation calculations. Dynamically modified windows, J. Chem. Phys. 90:2460–2470, 1989.
33. van Gunsteren, W. F., Berendsen, H. J. C. Thermodynamic cycle integration by computer simuilation as a tool for obtaining free energy differences in molecular chemistry. J. Computer Aided Mol. Des. 1:71–176, 1987.
34. Ferguson, D. M., Pearlman, D. A., Swope, W. C., Kollman, P. A. Free energy perturbation calculations involving potential function changes. J. Comput. Chem. 13:362–370, 1992.
35. Wade, R. C., Mazor, M. H., McCammon, J. A., Quiocho, F. A. A molecular dynamics study of thermodynamic and structural aspects of the hydration of cavities in proteins. Biopolymers 32:919–931, 1991.
36. van Eerden, J., Harkema, S., Feil, D. Molecular dynamics of 18-crown-6 complexes with alkali metal cations: Calculation of relative free energies of complexation. J. Phys. Chem. 92:5076–5079, 1988.
37. Hendrickson, W. A., Påhler, A., Smith, J. L., Satow, Y., Merritt, E. A., Phizackerley, R. P. Crystal structure of core steptavidin determined from multiwavelength anomalous diffraction of syncrotron radiation. Proc. Natl. Acad. Sci. U.S.A. 86:2190–2194, 1989.
38. Mizushima, N., Spellmeyer, D., Hirono, S., Pearlman, D., Kollman, P.A. Free energy perturbation calculations on binding and catalysis after mutating threonine 220 in subtilisin, J. Biol. Chem. 266:11801–11809, 1991.
39. Caldwell, J. W., Agard, D. A., Kollman, P. A. Free energy calculations on binding and catalysis by α-lytic protease: The role of substrate size in the P_1 pocket. Proteins 10: 140–148, 1991.
40. (a) Hirono, S., Kollman, P. A. Calculation of the relative binding free energy of 2′GMP and 2′AMP to ribonuclease T1 using molecular dynamics/free energy perturbation approaches. J. Mol. Biol. 212:197–209, 1990; (b) Hirono, S., Kollman, P. A. Relative binding free energy calculations of inhibitors to two mutants (Glu 46 → Ala/Gln) of ribonuclease T1 using molecular dynamics/free energy perturbation approaches. Protein Eng. 4:233–243, 1991.
41. Pearlman, D. A., Kollman, P. A. The calculated free energy effects of 5 methyl cytosine on the B to Z transition in DNA. Biopolymers 29:1193–1209, 1990.
42. Ferguson, D. M., Radmer, R. J., Kollman, P. A. Determination of the relative binding free energies of peptide inhibitors to the HIV-1 protease. J. Med. Chem. 34:2654–2659, 1991.
43. Merz, K. M., Jr., Kollman, P. A. Free energy perturbation simulations of the inhibition of thermolysin: Prediction of the free energy of binding of a new inhibitor. J. Am. Chem. Soc. 111:5649–5658, 1989.
44. Richards, W. G., King, P. M., Reynolds, C. A. Solvation effects. Protein Eng. 2:319–327, 1989.
45. Besler, B. H., Merz, K. M., Jr., Kollman, P. A. Atomic charges derived from semi empirical methods. J. Comput. Chem. 11:431–439, 1990.
46. (a) Jorgensen, W. L., Pranata, J. Importance of secondary interactions in triply hydrogen bonded complexes: Guanine-cytosine vs uracil-2,6 diaminepyrimidine. J. Am. Chem. Soc. 112:2008–2010, 1990; (b) Pranata, J., Wierschke, S. G., Jorgensen, W. L. OPLS potential functions for nucleotide bases. Relative association constants of hydrogen-bonded base pairs in chloroform. J. Am. Chem. Soc. 113:2810–2819, 1991.
47. Doig, A. J., Williams, D. H. Binding energy of an amide-amide hydrogen bond in aqueous and nonpolar solvents. J. Am. Chem. Soc. 114:338–343, 1992.
48. Miyamoto, S., Kollman, P. A. What determines the strength of non-covalent associations of ligands to proteins. Proc. Nat. Acad. Sci. U.S.A., submitted.
49. (a) Warshel, A., Sussman, F., Hwang, J.-K. Evaluation of catalytic free energies in genetically modified proteins. J. Mol. Biol. 201:139–159, 1988; (b) Dang, L. X.; Kollman, P.A. Free energy of association of the 18-crown-6:K^+ complex in water: A molecular dynamics simulation. J. Am. Chem. Soc. 112:5716–5720, 1990.
50. Brooks, C. L., III, Fleischman, S. H. A theoretical approach to drug design: 1. Relative solvation thermodynamics for the anti-bacterial compound trimethoprim and ethyl derivatives substituted at the 3′, 4′ and 5′ positions. J. Am. Chem. Soc. 112:3307–3312, 1990.